ACS OMEGA

Open Access

http://pubs.acs.org/journal/acsodf

Article

Synthesis of Novel (Meth)acrylates with Variable Hydrogen Bond Interaction and Their Application in a Clear Viscoelastic Film

Weizhong Xiang and Jianhui Xia*

Cite This: *ACS Omega* 2024, 9, 13644−13654

Read Online

ACCESS | Metrics & More | Article Recommendations | Supporting Information

ABSTRACT: Clear viscoelastic films (CVFs) have many applications in the display industry. Acrylic monomers containing a hydrogen bond (H-monomer) are often used in the preparation of CVF to increase the cohesion and form favorable interactions with the display substrate. Common H-monomers face a counterbalance between the glass transition temperature (T_g) and the hydrogen-bonding association constant (K_a). Strong hydrogen bonding often leads to a high T_g and high modulus, which are unfavorable in certain applications such as foldable display. To solve these problems, four types of hydrogen-bonding (meth)acrylic monomers (carbamate acrylate, carbamate methacrylate, urea acrylate, and urea methacrylate) with different K_a and T_g were readily synthesized. Among them, urea acrylates displayed the highest K_a while still maintaining moderate T_g. These H-monomers were copolymerized with 2-ethylhexyl acrylate (EHA) and cross-linked to obtain a series of copolymers (H-copolymers) as pressure-sensitive adhesives. After the characterization of rheology, optics, and peel adhesion, urea-acrylic H-copolymers showed the best overall performance by combining great optical property (>98% in transmittance, < 1% in haze) and mechanical performance (8−12 N/25 mm in peel adhesion, 84−92% in creep recovery). This work provides a new path to prepare acrylic CVF for flexible display application.

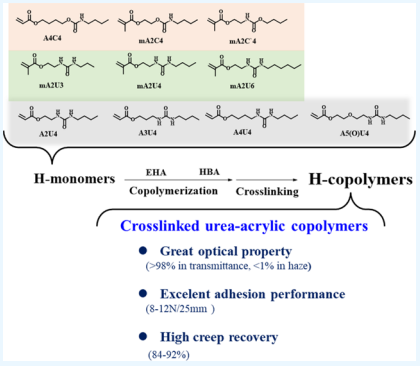

INTRODUCTION

In recent years, the development of display technology has made great progress, gradually changing from rigid to flexible format, such as a foldable display. The display module is a multilayer device composed of various functional layers and bonded by the clear viscoelastic film (CVF).[1−4] CVF is an optically clear polymer with balanced viscoelasticity properties, namely, having sufficient flow (viscosity) to fully wet the surface of the adherend while having good cohesive strength (elasticity) to fix the adherend as well. For foldable display, CVF plays an essential role of enabling a robust flexible display by optimizing the folding mechanics, as all other functional layers (e.g., the light source, electrode, and sensor) are usually hard or brittle materials.[1] High transmittance, good bonding, high recovery, and temperature-stable properties are essential for foldable CVF application.

(Meth)acrylic polymers are popular in the preparation of CVF due to their advantages such as weather resistance and light transmittance.[5] A common approach to designing polyacrylate-based CVF materials is by copolymerizing low-T_g monomers such as butyl acrylate (BA)[6] and 2-ethylhexyl acrylate (2-EHA)[7,8] with acrylates containing hydrogen bonds,[9,10] dynamic chemical bonds,[11,12] and coordination bonds[13] to yield the final polymer with both adhesiveness and elasticity. The former provides the lower modulus and fluidity required for adhesives; the latter provides energy dissipation, recovery, and even self-healing,[14] shape memory,[15,16] and photothermal reversible properties[17−19] by secondary bonding interactions.

When a hydrogen bond interaction is introduced into CVF, there is a balance among solubility, hydrogen bond strength (K_a), and glass transition temperature (T_g). Strong hydrogen bonds (such as the quadruple hydrogen bond UPy[11,17,20,21]) can only be dissolved in a high-boiling-point solvent, which is not conducive to the preparation of pressure-sensitive adhesive materials. For commonly used monomers in the market, such as hydroxyethyl acrylate (HEA),[22,23] acrylic acid (AA),[7,8] and acrylamide (ACM),[24] there is a conflict between low T_g and high K_a: low-T_g monomers such as HEA and hydroxy butyl acrylate (HBA) have weak hydrogen bond strength, which hardly meet the mechanical and recovery requirements unless the cross-linking density is improved.[23] However, high-T_g monomers such as acrylic acid and acrylamide with relatively high hydrogen bond strengths would increase the elastic modulus or incur phase separation during copolymerization and impair optical transmittance.

Received: October 2, 2023
Revised: January 25, 2024
Accepted: February 5, 2024
Published: March 16, 2024

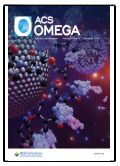

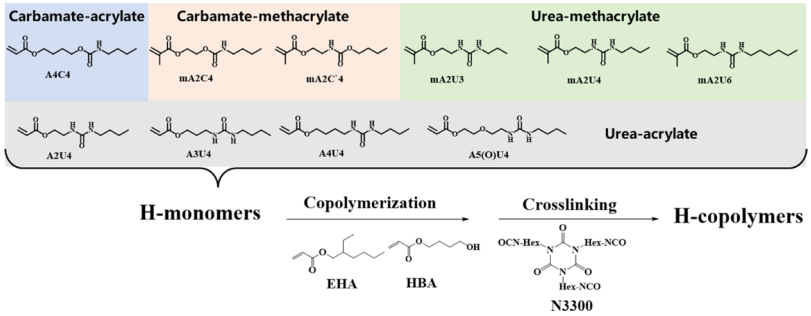

Figure 1. List of (meth)acrylates with variable side-chain hydrogen bond interaction and the schematic synthetic route for making the copolymers (H-copolymers).

For foldable display application, it is desirable to develop CVF with a high hydrogen bond strength for good recovery and low T_g for wide-temperature application. To address the conflict of high hydrogen bond strength and low T_g in commercial acrylic monomers, we synthesized a series of (meth)acrylic monomers with variable hydrogen bond interaction and studied their application in foldable CVF (Figure 1). Specifically, we introduced carbamate and urea moieties into the (meth)acrylic side chain to adjust the hydrogen bond strength. Generally, carbamate and urea groups often exist in main-chain polymers like polyurethane and polyurea[25−27] to improve the toughness and adhesion of materials.[28,29] For polyacrylates with side-chain carbamate or urea groups, a greatly increased polymerization rate[30,31] or self-healing properties[14] have been reported. In addition, Cao et al. used an acrylic polymer with a carbamate side group to blend with commercial adhesives, and obtained a kind of adhesive with self-healing properties and ultrahigh toughness.[14] Liu et al. made an *N*-allyl thiourea-containing copolyacrylate with temperature-insensitive viscoelasticity and reported its versatile usage in water and oil by the hydrogen-bond interaction between *N*-allyl thiourea and 2-methoxyethyl group.[32] Sada et al. prepared a side-chain polyacrylate containing a urea group using the RAFT polymerization method. Using the thermal reversibility of the urea hydrogen bond, the transmittance was changed by changing the temperature of the polymer solution.[33] Long et al. prepared a block copolymer of a methacrylate-containing urea group inside a chain with other monomers and studied its self-assembly and self-healing behavior by using the reversibility of the urea hydrogen bond.[34,35]

Additionally, Inspired by Weder and Mejier's work of introducing a long chain between the hydrogen bond-containing group and the vinyl group to reduce the glass transition temperature and improve the solubility,[17,18,21] different spacer groups were induced between the (meth)-acrylic moiety and the carbamate/urea group to reduce their polymer T_g while preserving their hydrogen-bond interactions. The hydrogen bond association constants K_a of different monomers were obtained by the hydrogen titration experiment via ^{1}H NMR spectra.[36,37] The relationship between the polymer's T_g and the monomer's K_a was established. Copolymers of these (meth)acrylates with variable hydrogen bond interactions were prepared, and their use as foldable CVF was studied. To the best of our knowledge, this is the first report of applying adjustable side-chain hydrogen bond (meth)acrylates in a foldable display application.

RESULTS AND DISCUSSION

As stated earlier, the aim of this article is to obtain a foldable CVF with high hydrogen bond strength and low T_g. To achieve this, we synthesized different side-chain carbamate and urea (meth)acrylates with various spacers between the hydrogen bond-containing group and the vinyl group (Figure 1). The polymerization of these side-chain hydrogen bond (meth)-acrylates and their foldable CVF properties were studied.

All H-monomers in Figure 1 were synthesized successfully (see Figures S1−S14 for ^{1}H NMR and ^{13}C NMR) and denoted by abbreviations based on the functional groups they contain: (1) **A** and **mA** stand for acrylate and methacrylate, and **U** and **C** stand for the urea and carbamate groups; (2) the numbers between **A** (or **mA**) and **U** (or **C**) or behind **U** (or **C**) represent the atomic number of middle and end groups, respectively; and (3) because of the asymmetry of the carbamate groups, C and C′ are used for structure −O−CO−NH− and structure −NH−CO−O−, respectively. Taking 2-(2-(3-butylureido)ethoxy)ethyl acrylate (A5(O)U4) for example, **A** and **U** indicate acrylate and urea groups, while 5(O) and 4 stand for the ethoxyethane group (between **A** and **U**) and butyl end group (behind **U**), respectively.

Polymerization of Side-Chain Carbamate and Urea (Meth)acrylates. The choice of solvent is important to carry out the solution polymerization homogeneously, especially when polymers with high molecular weight are targeted. For carbamate methacrylate, ethyl acetate (EA) was used as the solvent. As shown in Figure 2, for urea-containing (meth)-acrylates, ethyl acetate alone or a mixture of ethyl acetate/methanol (MeOH) led to gelation or low molecular weight, while a mixed solvent of ethyl acetate (EA)/*N*,*N*-dimethylformamide (DMF) (7/3 weight ratio) was found to be appropriate for the homogeneous copolymerization of urea-containing monomers.

The molecular weight information and the thermal stability of the synthesized H-copolymers are shown in Table 1. The subscript numbers of the copolymers represent the molar feed ratio, and **E** and **H** represent the EHA and the HBA monomers, respectively. Taking the item "A4C4$_{10}$E$_{90}$H$_2$" in Table 1 as an example, it indicates that the copolymer is obtained by polymerization of monomers A4U4, EHA, and HBA in a molar ratio of 10/90/2. Gel permeation chromatography (GPC) results showed that the weight-average molecular weight (M_w) is between 400 and 600 kDa and polydispersity (PDI) is between 3 and 6 (see Figure S23 in SI for detailed data). For thermal stability, the decomposition temperature of $T_{d1\%}$ (defined as the temperature at which 1% of the initial sample mass was lost) was obtained from the

https://doi.org/10.1021/acsomega.3c07566
ACS Omega 2024, 9, 13644−13654

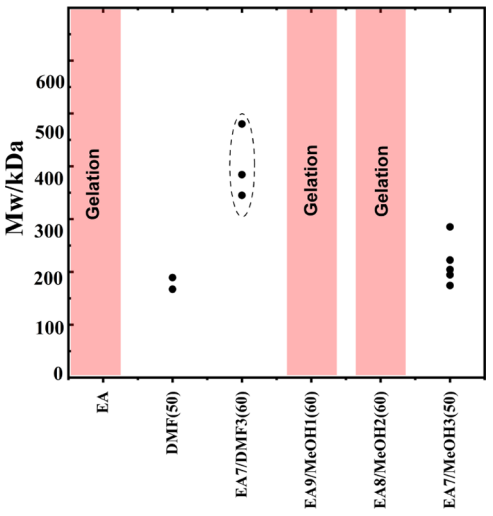

Figure 2. M_w of urea-methacrylic copolymers (mA4U4$_{10}$E$_{90}$) obtained in different solvents. (The number in parentheses on the horizontal coordinate indicates the mass concentration of the monomers.)

Table 1. Weight-Average Molecular Weight, Polydispersity, and Chemical Composition of H-Copolymers

copolymers[a]	M_w (kDa)[b]	PDI[b]	$T_{d1\%}$ (°C)[c]	H-monomers (mol %)[d]
A4C4$_{10}$E$_{90}$H$_2$	532.3	3.02	230	12
mA2C′4$_{10}$E$_{90}$H$_2$	657.5	5.94	290	10
mA2C4$_{10}$E$_{90}$H$_2$	584.3	4.86	275	10
mA2U3$_{10}$E$_{90}$H$_2$	495.6	4.95	236	9
mA2U4$_{10}$E$_{90}$H$_2$	533.2	3.95	230	10
mA2U6$_{10}$E$_{90}$H$_2$	407.9	3.57	237	11
A2U4$_{10}$E$_{90}$H$_2$	468.3	4.00	235	10
A3U4$_{10}$E$_{90}$H$_2$	556.7	4.46	213	12
A4U4$_{10}$E$_{90}$H$_2$	626.6	4.96	232	10
A5(O)U4$_{10}$E$_{90}$H$_2$	476.0	4.23	224	12

[a]The numerical subscript represents the mole fraction of each component. [b]It was tested by gel permeation chromatography. [c]Obtained by thermogravimetric analysis test, where "1%" represents 1% of the lost sample mass, and is defined as the decomposition temperature. [d]The results were calculated by ^{1}H NMR spectroscopy.

thermogravimetric analysis (TGA, see SI, Figure S16 for specific results). Consistent with the previous report,[38] the TGA results showed two stages, with the first one being the decomposition of the carbamate or the urea moiety (about 280 and 220 °C, respectively), and the second one being the decomposition of the (meth)acrylate main chain (about 300 °C).

Table 1 also lists the chemical composition of the copolymers. The composition was calculated by the integral ratio of the proton on the methylene group of −COO−C**H**$_2$− and −CO−NH−C**H**$_2$− in the ^{1}H NMR spectra. The representative ^{1}H NMR spectra and chemical structures of mA2C′4, mA2C4, and mA2U4-based copolymers are shown in Figure 3. The chemical shift at δ = 3.95 ppm represents the −COO−C**H**$_2$−, which exists in both the H-monomers, EHA and HBA, while the chemical shift of the −CO−NH−C**H**$_2$− from δ = 3.05 to 3.55 ppm belongs exclusively to H-monomers. Then, the composition of the H-monomer in copolymers can be calculated by the integral area's ratio of δ = 3.45 ppm (Figure 3a) or δ = 3.15 ppm (Figure 3b,c) for −CO-NH−C**H**$_2$− to δ = 3.95 ppm for −COO−C**H**$_2$−, which are recorded in Table 1 (H-monomers (mol %)).

Additionally, the chemical shift at δ = 3.65 ppm belongs to −C**H**$_2$−OH at HBA and chemical shifts higher than δ = 4.05 ppm represent the −NH−COO−C**H**$_2$− in carbamate-based H-monomers (Figure 3a,b). It was found that the compositions of all of the copolymers (see SI for the ^{1}H NMR spectra of other copolymers, Figures S17−S19) were in good agreement with the feed ratio.

Calculation of K_a and Its Correlation with T_g. Using ^{1}H NMR spectroscopy to calculate the hydrogen-bond association constant (K_a) is a mature method and has been widely used.[34,37,39,40] It assumes that the association of the hydrogen-bond donor and acceptor will reach an equilibrium, and the concentration of acceptor−donor dipole will affect the chemical shift of the protons involved in forming the hydrogen bond. Based on these assumptions, a formula with a clear physical meaning can be derived and fitted using experimental data to get K_a (see Methods Section and Supporting Information (SI) for specific formulas and derivations). Using monomer A4U4 as an example (other ^{1}H NMR data of H-monomers are shown in Figure S20), the chemical shift change of acrylate-N**H**-*co*-NH− was recorded using different initial monomer concentrations in Figure 4a, and the hydrogen bond association strength of A4U4 could be calculated by formula fitting as shown in Figure 4b.[36,37] The high correlation coefficient of R^2 = 0.997 indicated that the experimental data conformed well with the theoretical formula.

The relationship of H-polymer's T_g and its monomer's K_a is shown in Figure 5 (see Figure S15 for T_g measured by DSC, and Table S1 for K_a calculated by ^{1}H NMR). The T_g and K_a

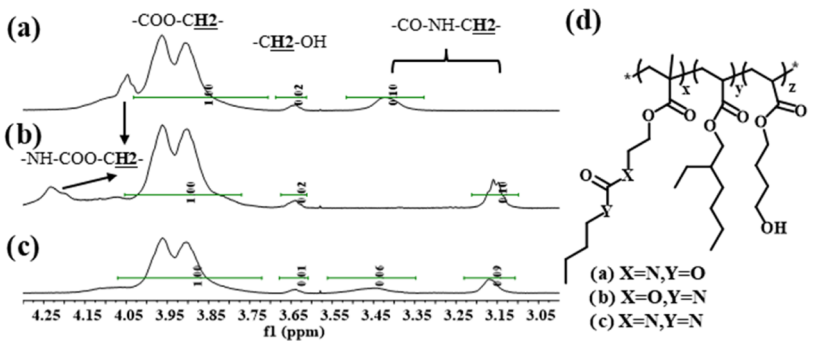

Figure 3. ^{1}H NMR spectra of copolymers of (a) mA2C′4$_{10}$E$_{90}$H$_2$, (b) mA2C4$_{10}$E$_{90}$H$_2$, and (c) mA2U4$_{10}$E$_{90}$H$_2$; (d) chemical structures of the copolymers.

https://doi.org/10.1021/acsomega.3c07566
ACS Omega 2024, 9, 13644−13654

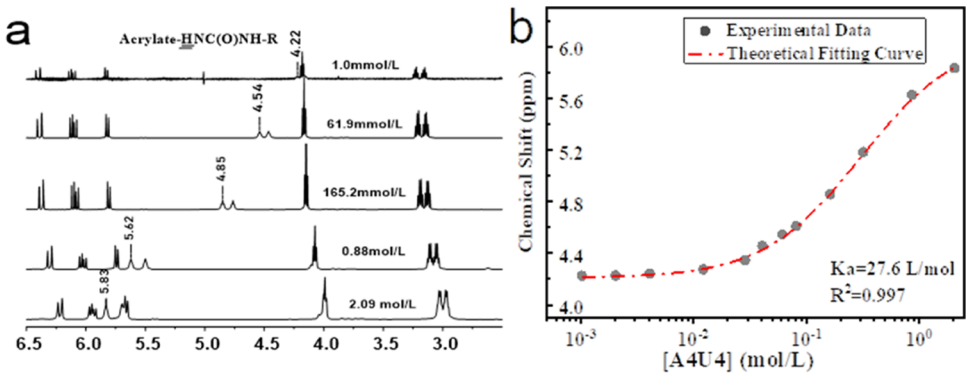

Figure 4. Chemical shift of −HNCONH− in A4U4 monomer with the [A4U4] changing from 0.001 to 2 mol/L, (a) ^{1}H NMR spectra, and (b) corresponding data plot.

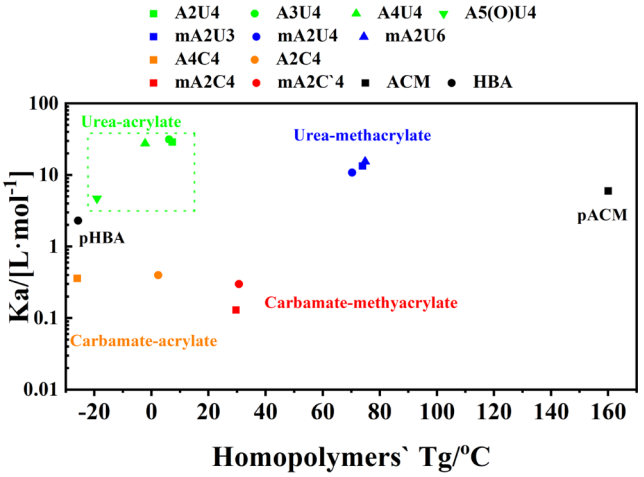

Figure 5. Plot of hydrogen-bond association constant K_a and glass transition temperature T_g.

experimental data of ACM and HBA, which are commonly used in CVF, were also measured for comparison. As can be seen in Figure 5, H-monomers containing the urea group had the highest K_a. Furthermore, the hydrogen-bond association constant K_a was mainly determined by the type of the hydrogen bond (>10 L/mol for the urea group and <0.5 L/mol for the carbamate group). The introduction of ether on the side group (e.g., A5(O)U4) or methyl group (mA2U3, mA2U4, mA2U6) on the vinyl group could inhibit the formation of intermolecular hydrogen bonds and afford lower K_a.[21] The T_g was mainly determined by the main chain, with polymethacrylate having a higher T_g than polyacrylate. The hydrogen bond on the side chain also had some effect on T_g, and the T_g of the urea-based copolymers was found to be higher than that of the carbamate-based copolymers. Furthermore, the flexibility of the spacer between the side-chain hydrogen-bond group (urea or carbamate) and the (meth)acrylic ester had a great effect on the T_g. As the flexibility of the spacer increased, T_g dropped dramatically from 7 °C (A2U4) to −20.6 °C (A5(O)U4) and from 2.9 °C (A2C4) to −26.0 °C (A4C4). However, the length of the end alkyl group (mA2U3, mA2U4, and mA2U6) or the configuration of the carbamate group (mA2C′4, mA2C4) had little effect on T_g. Compared with commercially available monomers that contain strong hydrogen bonds (e.g., ACM), the synthesized urea acrylate had a higher hydrogen bond interaction and lower T_g.

Rheology Test. The results of the rheological temperature sweep and creep recovery test before and after cross-linking of H-copolymers are shown in Figure 6 and Table 2 and the subscript number of **N** in Figure 6 and Table 2 indicates the mass percentage of N300 added for cross-linking. After cross-linking, the storage modulus G ′ and creep recovery of H-copolymers increased, because of the high gel fraction of the cross-linked network (e.g., > 70% in Table 2). The T_g of the copolymers was obtained by the peak value of tan δ in Figure 6 and the results are listed in Table 2.

The copolymers of EHA with carbamate-containing monomers (A4C4, mA4C4, and mA4C′4) displayed one T_g (Figure 6a). However, phase separation was observed for the copolymers of the urea-containing monomer. All urea-containing methacrylic copolymers showed phase separation (Figure 6c). For urea-containing acrylic copolymers, phase separation occurred only with A4U4 (Figure 6e). Presumably, phase separation was the result of reactivity ratio difference. It has been previously reported that urea monomers have a higher competition rate in copolymerization.[30,31,41] Furthermore, methacrylates typically have higher reactivity ratios than acrylates.

The creep recovery before and after cross-linking (Figure 6b,d,f and Table 2) showed that cross-linking had a significant impact on the creep recovery performance especially for carbamate-containing (weaker hydrogen bond interaction) copolymers. The urea-containing copolymers with a stronger hydrogen bond interaction had better creep recovery than carbamate-containing copolymers before cross-linking.

The cross-linking of the copolymers was studied by the addition of the N3300 cross-linker. Except for A5(O)-$U4_{10}E_{90}H_2N_{0.15}$, high gel content was obtained. The low gel content of $A5(O)U4_{10}E_{90}H2N_{0.15}$ agreed with the high tan(δ) value in the rheology characterization (Figure 6e). Nevertheless, chain entanglement was increased after the addition of N3300, as evident in the decreased tan(δ) (Figure 6e) and increased creep recovery (Figure 6f). Both the hydrogen bond and chemical cross-linking led to increased creep recovery, and the stronger hydrogen bond of urea contributed more to the recovery.

According to Dahlquist's criterion, the adhesive film remains pressure sensitive when the storage modulus (G') is below 10^5 Pa.[42] Here, the minimum temperature at which G' is below the Dahlquist criterion (<10^5 Pa) is defined as T_{min}, which roughly indicates the lowest temperature at which the polymer is pressure-sensitive and can reflect its low-temperature resistance as a CVF. As shown in Table 2, T_{min} correlates well with T_g.

https://doi.org/10.1021/acsomega.3c07566
ACS Omega 2024, 9, 13644−13654

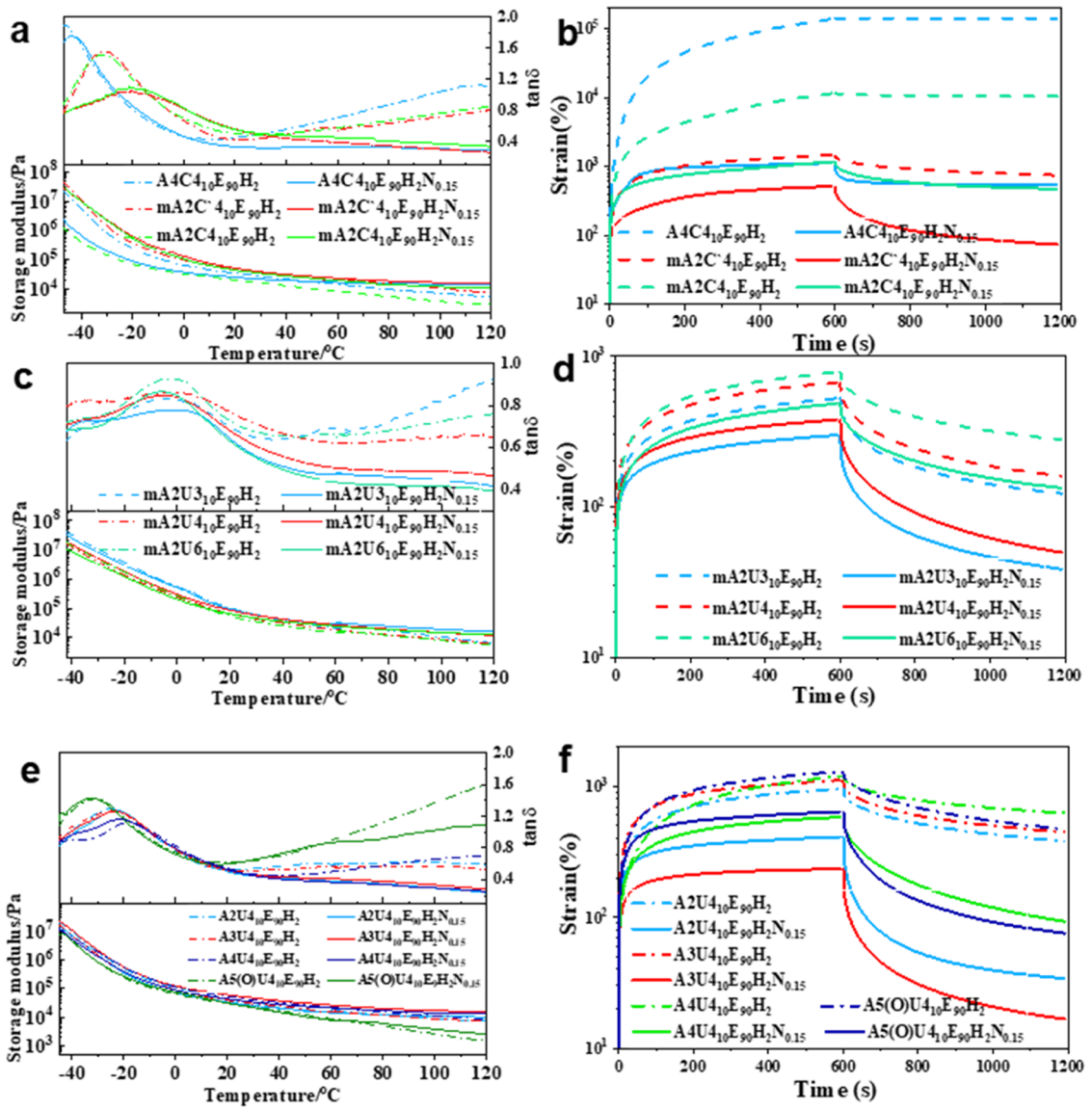

Figure 6. Variation of (a, c, e) tan δ/storage modulus G' with temperature and (b, d, f) creep test for (a, b) carbamate-polyacrylate and carbamate-poly(meth)acrylate, (c, d) urea-poly(meth)acrylate, and (e, f) urea-polyacrylate.

Table 2. Rheology Characteristics and Gel Content Test of Cross-linked H-Copolymers

cross-linked H-copolymers	T_g (°C)[a]	creep recovery (%)[b]	T_{min} (°C)[c]	E_a (kJ/mol)[d]	gel content (%)[e]
A4C4$_{10}$E$_{90}$H$_2$N$_{0.15}$	−43.9	0.4 → 52.0	−21.6	59.3	82.9
mA2C'4$_{10}$E$_{90}$H$_2$N$_{0.15}$	−21.8	48.6 → 85.5	4.3	60.7	90.4
mA2C4$_{10}$E$_{90}$H$_2$N$_{0.15}$	−24.0	10.6 → 59.9	1.0	63.3	88.0
mA2U3$_{10}$E$_{90}$H$_2$N$_{0.15}$	−37.0/−1.6	76.8 → 87.2	18.7	89.8	93.8
mA2U4$_{10}$E$_{90}$H$_2$N$_{0.15}$	−35.6/−5.2	76.2 → 87.0	16.3	69.5	87.4
mA2U6$_{10}$E$_{90}$H$_2$N$_{0.15}$	−38.0/−5.9	64.7 → 72.8	10.1	69.8	70.3
A2U4$_{10}$E$_{90}$H$_2$N$_{0.15}$	−22.3	63.7 → 91.7	−6.4	64.5	86.5
A3U4$_{10}$E$_{90}$H$_2$N$_{0.15}$	−23.6	59.8 → 92.3	4.1	65.7	93.2
A4U4$_{10}$E$_{90}$H$_2$N$_{0.15}$	−39.4/−21.4	52.0 → 84.1	−2.9	79.0	81.8
A5(O)U4$_{10}$E$_{90}$H$_2$N$_{0.15}$	−32.6	60.1 → 87.4	−6.7	68.7	<5

[a]Obtained by temperature swipe experiment in a rheometer. [b]Obtained by creep recovery experiment in the rheometer before and after cross-linking. [c]T_{min} defined as the minimum temperature where the $G' < 10^5$ Pa in sweep temperature experiment. [d]E_a was calculated via Arrhenius formula in the time−temperature superposition (TTS) spectra of the frequency scan experiment. [e]Obtained by gel fraction test.

The time−temperature superposition (TTS) frequency spectra of all un-cross-linked H-copolymers were analyzed by the WLF equation. The polynomial fitting curves are shown in Figure 7 (see Figure S21 for raw data) and the apparent flow activation energy E_a was calculated (Table 2). In Figure 7a−c, none of the un-cross-linked H-copolymers exhibited the

https://doi.org/10.1021/acsomega.3c07566
ACS Omega 2024, 9, 13644−13654

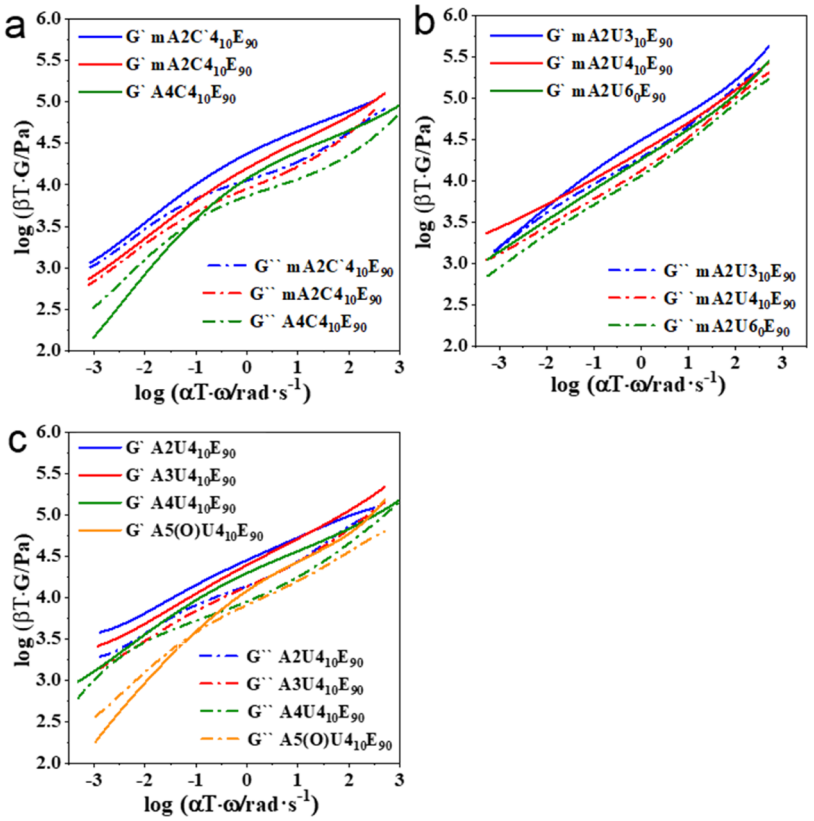

Figure 7. Polynomial fitting master curves of un-cross-linked (a) carbamate-containing copolymers (polyacrylate and polymethacrylate), (b) urea-containing methacrylic copolymers, and (c) urea-containing acrylic copolymers.

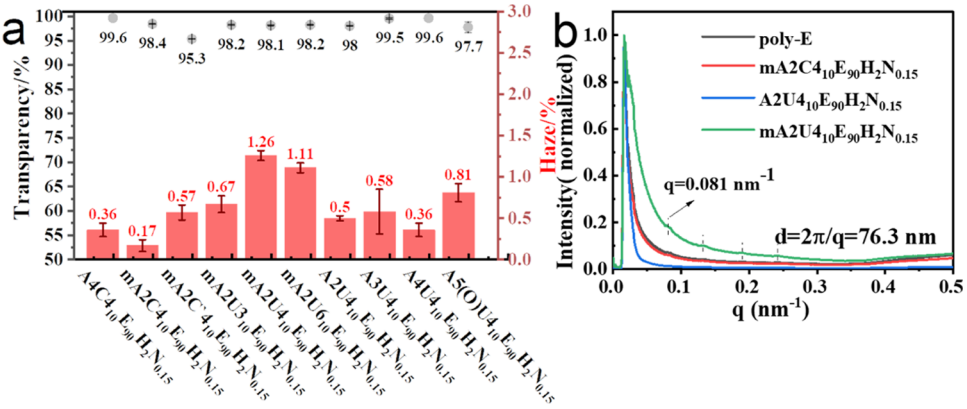

Figure 8. (a) Transmittance and haze results of all cross-linked H-copolymers and (b) SAXS spectra of poly-E, mA2C4$_{10}$E$_{90}$N$_{0.15}$, A2U4$_{10}$E$_{90}$N$_{0.15}$, and mA2U4$_{10}$E$_{90}$N$_{0.15}$.

rheological behavior of the typical Maxwell viscoelastic model. In addition, most of the copolymers showed $G' > G''$ at low frequency (<0.01 Hz). This was attributed to the uneven distribution of monomers along the polymer main chain, together with the large molecular weight (Mw around 500 kDa) and high polydispersity (PDI around 4) of the copolymers.[43] In the study of Mitchell Anthamatten et al., it was shown that when polymer Mw was low (30 kDa) and PDI was narrow (around 2), poly(acrylic acid-*co*-butyl acrylate) and poly(butyl acrylate) both satisfied the Maxwell viscoelastic model.[32,44] Higher Mw (600 kDa) and broader PDI (around 4) resulted in deviation from the Maxwell viscoelastic model (See SI, Figure S22), and were shown to follow the Sticky Rouse model.[45−47]

Transmittance/Haze and Adhesion Force Test. Copolymer films 50 um thick have almost no obvious difference in transmittance and haze under the naked eye (Figure S24). The transmittance and haze data of all cross-linked H-copolymers with a film thickness of 50 μm (μm) are shown in Figure 8a. High transmittance and low haze were obtained for all samples, except the urea-containing methacrylic copolymers, which showed a higher haze. This is mainly due to microphase separation. In Figure 8b (small-angle X-ray scattering experiment (SAXS)), the urea methacrylate copolymer (mA2U4$_{10}$E$_{90}$H$_2$N$_{0.15}$) displayed a microphase separation with a domain size less than 100 nm, which resulted in a slightly increased haze. This is attributed to the difference of the monomer's reactivity in copolymerization.

https://doi.org/10.1021/acsomega.3c07566
ACS Omega 2024, 9, 13644−13654

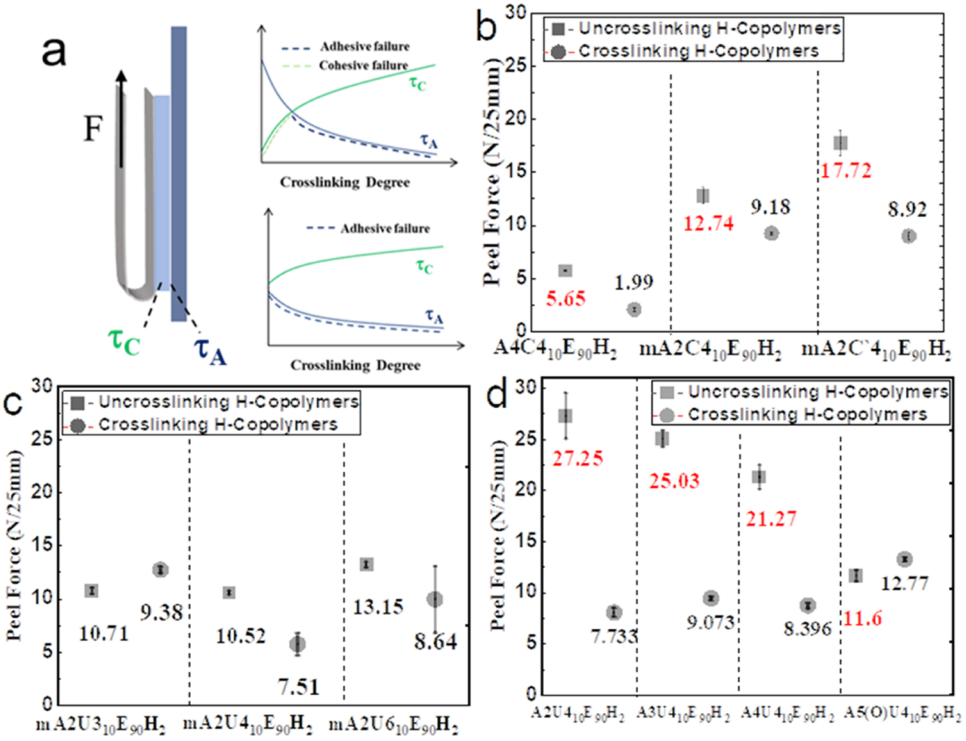

Figure 9. (a) Schematic diagram of the peel adhesion test and failure pattern; peel adhesion results of (b) carbamate-containing copolymers, (c) urea-containing methacrylic copolymers, and (d) urea-containing acrylic copolymers before (square) and after (dot) cross-linking.

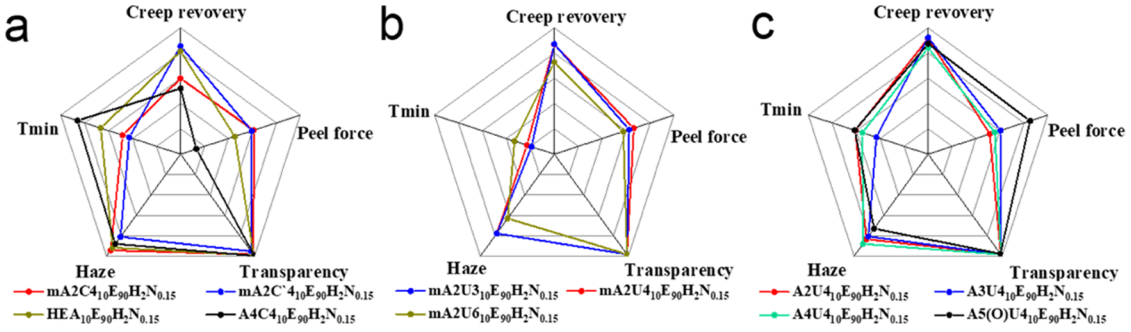

Figure 10. Radar chart of comprehensive performance with (a) carbamate-based copolymers, (b) urea-methacrylic copolymers, and (c) urea-acrylic copolymers. The ranges are $T_{min} \in [-30, 30]$ °C, creep recovery ∈ [0, 100] %, peel adhesion ∈ [0, 15]N/25 mm, transmittance ∈ [0, 100]%, and haze ∈ [3, 0]%.

The greater the difference in polymerization rates between the H-monomer and 2-ethylhexyl acrylate (EHA), the more likely phase separation (or microphase separation) is to occur. The higher reactivity ratio of methacrylate compared to arylate and the high hydrogen bond strength of the urea moiety lead to less uniform incorporation of the urea-containing methacrylate in the copolymerization. As a result, (micro)phase separation is more likely to occur in the urea-containing methacrylic copolymers.

The adhesion behavior is directly related to the viscoelastic properties of the film: high elasticity often leads to the increase of cohesion stress (τ_C) in bulk, while high viscosity can improve the adhesive stress (τ_A) in the interface between the adhesives and the adherend.[48] The result of the peeling force test is determined by the relative strengths of τ_C and τ_A, which determines the cohesive failure ($\tau_C > \tau_A$), adhesive failure ($\tau_C < \tau_A$), or mixture failure ($\tau_C \approx \tau_A$).[49]

Figure 9b–d shows the 180° peel adhesion results before and after the cross-linking (a 0.15 wt % N3300 cross-linker was used for all cross-linked samples as mentioned above), where cohesion failure is marked red and adhesion failure is marked black. Chemical cross-linking led to the increase of τ_C and the decrease of τ_A, as the ability of the adhesive to infiltrate the interface was weakened (Figure 9a). In general, before chemical cross-linking, for carbamate-containing copolymers (Figure 9b) and urea-containing acrylic copolymers (Figure 9d), τ_C was smaller than τ_A ($\tau_C < \tau_A$) and this led to cohesive failure. After cross-linking, adhesive failure happened ($\tau_C > \tau_A$). However, for urea-containing methacrylic copolymers (Figure 9c), the cohesion stress was higher than the adhesion stress ($\tau_C > \tau_A$) before cross-linking and no cohesive failure was observed before and after cross-linking. Overall, urea-acrylic copolymers had balanced adhesive properties.

Comprehensive Assessment. Optical property (transmittance and haze), mechanical properties (creep recovery, peel adhesion, recovery properties), and service temperature (T_{min}) of adhesives are important considerations in foldable CVF. Figure 10 summarizes the comprehensive properties of

https://doi.org/10.1021/acsomega.3c07566
ACS Omega 2024, 9, 13644−13654

the four types of H-copolymers with 25 mm width and 50 μm thickness (carbamate-based copolymers in Figure 10a, urea-methacrylic copolymers in Figure 10b, urea-acrylic copolymers in Figure 10c). It shows that carbamate-based copolymers had acceptable optical performance but poor mechanical properties (low creep recovery or peeling adhesion). For urea-methacrylic copolymers, phase separation resulted in increased haze (~1.5%) and high T_g yielded high T_{min} (>10 °C). In comparison, urea-acrylic copolymers had good optics, desirable mechanical properties, and a low T_{min}. This was attributed to the introduction of a strong hydrogen bond while still maintaining a low glass transition temperature.

CONCLUSIONS

In conclusion, different (meth)acrylic monomers forming the side-chain hydrogen bond were synthesized and their application in the preparation of CVF for foldable display was evaluated. The urea acrylate showed a high hydrogen-bonding association constant K_a and a moderate-low T_g. The K_a was mainly determined by the hydrogen-bonding group and the urea group had a higher K_a than carbamate. The glass transition temperature decreases when increasing the flexibility of the spacer between the main chain and the hydrogen-bond site at the side chain. The urea-acrylic copolymers showed the best overall properties, with a high transmittance (98.4%), low haze (0.36%), moderate peeling adhesion (8.36N), and high creep recovery (84.1%). This study provides a general method for synthesizing novel CVF materials.

METHODS

Materials. All the reactants with 97−99% purity and 2,2-azobis(2-methylpropionitrile) (AIBN) with 98% purity and anhydrous sodium sulfate (Na_2SO_4, > 99.0% purity) used for synthesis and polymerization are purchased from Adamas, unless otherwise stated specifically. Dichloromethane (99.5% purity), ethyl acetate (EA, 99.5% purity), Petroleum ether (60−90 °C boiling point, AR), *N*,*N*-dimethylformamide (DMF, 99.5% purity), were purchased from Greagent Company. Methyl ethyl ketone (MEK; AR grade) was purchased from Guangzhou Chemical Reagent Factory. Tetrahydrofuran (THF; > 99% purity) was purchased from Thermo Fisher Scientific. Desmodur N3300, a commercial product containing isocyanate oligomer of hexamethylene diisocyanate, was purchased from Bayer. All chemicals were used without further purification.

Synthesis of H-Monomers. A typical synthesis of urea- and carbamate-containing methacrylic monomers from alkyl alcohol (butanol) and amine reactants (propylamine, butylamine, and hexylamine) is as follows. A 100 mL round-bottom flask equipped with a magnetic stir bar was charged with one equivalent of liquid amine in 20 wt % in ethyl acetate (EA). One equivalent of 2-methacryloyloxyethyl isocyanate (MOI) was added dropwise with stirring at 0 °C (for propylamine, butylamine and hexylamine) or room temperature (for butanol) for 30 min, and then warmed slowly to room temperature (for propylamine, butylamine, and hexylamine) or 40 °C (for butanol) and stirred for an additional 12 h. EA was removed under reduced pressure, yielding a white powder solid(urea methacrylate) or colorless clear liquid (carbamate methacrylate) in >90% yield. For the synthesis of mA4C4 the procedure was the same except that butyl isocyanate was added dropwise to hydroxyethyl methacrylate.

For the reaction of urea-containing acrylic monomers, taking 3-(3-butylureido) propyl acrylate (A3U4) as an example: *n*-butyl isocyanate (9.91 g, 100 mmol) was added at vigorous stirring to a solution of 3-amino-1-propanol (7.51 g, 100 mmol) in EA/MeOH = 80:20 wt % mixture solvents (45 mL). The reaction mixture was stirred for one h at 0 °C and another 10 h at room temperature. The resulting solution was subjected to decreased pressure at 35 °C and washed with a mixture of EA/PE (petroleum ether) to obtain a white powder. To a solution of 1-butyl-3-(3-hydroxypropyl) urea (Product 2b in Figure S8) (8.71 g, 50 mmol) and triethylamine (5.57 g, 55 mmol) in dry dichloromethane (150 mL), acryloyl chloride (4.98 g, 55 mmol) was added dropwise at 0 °C and stirred for additional 10 h at room temperature. It was washed by $NaHCO_3$ (aq) and extracted by CH_2Cl_2 3 times and dried over anhydrous Na_2SO_4, followed by filtration and evaporation to dryness.

The detailed synthesis and the ^{1}H NMR spectra of all the above products are provided in the Supporting Information (SI, Figures S1−S14).

Homopolymerization, Copolymerization, and Cross-linking of H-Monomers. To obtain the T_g of the H-monomers, homopolymerizations were carried out. A representative procedure is as follows: ~2g of the H-monomer was first added to the reaction bottle, then 4 mL of solvent (ethyl acetate or DMF, depending on the monomers) was added, and nitrogen was bubbled in the bottle at 67 °C for 10 min. Then, 5 mg of azo-initiator among with small amount of solvent were injected and the mixture was allowed to react for 12 h. After the polymerization, the solution was concentrated by rotary evaporation, washed in ethanol 3 times and placed in a 65 °C vacuum oven for one night to obtain a white-thicky or powder-like polymer.

As for the copolymerization between H-monomers and EHA, copolymers were prepared by using the conventional free-radical copolymerization. The following is a representative procedure: 2-ethylhexyl acrylate (45 mmol) was first placed in a round-bottom flask. The H-monomer (5 mmol), HBA (1 mmol, 0.14 g) and solvents (EA or EA/DMF mixture, 50−60 wt % to all monomers) were sequentially added, and dry nitrogen was bubbled through the solution for 10 min under 67 °C at oil bath. After that, AIBN (0.1 wt %, ~10 mg) dissolved in 1 mL of EA was injected, and the reaction proceeded for 4−10 h. The copolymer was purified by precipitation in ethanol 3 times to yield a sticky white sticky material.

These copolymers were further cross-linked before the rheological, mechanical, and optical measurements. Thus, the copolymer was dissolved in ethyl acetate, followed by adding Desmodur N3300 (0.15 wt % of the copolymer). After the subsequent preparation of the membrane (see Transmittance/Haze and Adhesion Force Test Section), it was put into an oven at 80 °C for 16 h to obtain the cross-linked copolymer (reaction between −NCO in Desmodur N3300 and −OH in HBA).

Fabrication of H-Copolymers Films. The solid content (wt %) of the copolymer solution was obtained by measuring the residual mass of the copolymer solution after drying at 80 °C for 10 h. Then, N3300 at 0.15 wt % of copolymer was added, and the mixture was stirred for 16 h. After that, the film with a thickness of about 50 μm was obtained using a homemade lab comma coater with a notch bar and coating upon a poly(ethylene terephthalate) (PET) release film; the

https://doi.org/10.1021/acsomega.3c07566
ACS Omega 2024, 9, 13644−13654

thickness between the coated molds (h) could be obtained by the empirical formula $h = L/\text{wt \%} \times 1.5$, where L is the target film thickness of 50 μm. The thickness test was performed using dial thickness gauges (Mitutoyo, 547−400S). Then, another PET release film was covered upon the double layers and formed a sandwiched structure for further transmittance, haze, and peel adhesion tests.

For rheology characterizations, samples with an approximate thickness of 1000 μm were made by repeated folding before full cross-linking.

Characterization. *Composition and Thermal Properties.* Molecular weights and molecular weight distributions were measured by gel permeation chromatography (GPC; Waters 2707) with THF as the eluent (1.0 mL/min) and a refractive index detector. Nuclear magnetic resonance (^{1}H NMR, ^{13}C NMR) spectra were used to analyze the structure of H-monomers and composition of H-copolymers using the Bruker AV 500 NMR spectrometer. Thermogravimetric analysis (TGA) measurement was performed by utilizing an alumina crucible on TGA 5500 (TA Instruments) at a scanning rate of 10 °C/min from 30 to 500 °C under flowing nitrogen (25 mL/min). The T_g of H-homopolymers was measured via differential scanning calorimetry (DSC) measurements from −30 to 120 °C with a heating (cooling) rate of 10 °C/min by DSC 2500 (TA Instruments) and the T_g was obtained from the second heating curve.

^{1}H NMR Titration Experiments and Calculation of K_a. K_a was determined by a dilution titration followed by ^{1}H NMR spectroscopic analysis. Various concentrations of H-monomers (U_0) and their chemical shift (δ_{sample}) of −N<u>H</u>−CO−N<u>H</u>− in urea or −O−CO−N<u>H</u>− in the carbamate group were analyzed by the equation below according to the references[34,37,39,40]. The δ_{mono} and δ_{dimer} in the formula are the chemical shifts of free and completely bonded −N<u>H</u>−CO− in H-monomers ($J = \delta_{dimer} - \delta_{mono}$). The specific derivation process can be found in the Supporting Information (SI). All H-monomers, $CDCl_3$, and glassware were dried before the analysis.

$$U_0 = \frac{(\delta_{sample} - \delta_{mono})[J + (\delta_{sample} - \delta_{mono})]}{K_a[J - (\delta_{sample} - \delta_{mono})]^2}$$

Transmittance/Haze Measurement and Peel Adhesion Test. Transmittance and haze measurements were performed via Haze gard i 4775 (BYK-Gardner, German). All H-copolymer films with 50 μm thickness were cut into 5 cm × 5 cm slides, attached to the glass substrate for the measurement of transmittance/haze at four different sample sites and normalized by subtracting the signals from the substrate glass.

The 180° peel adhesion test was performed according to the ASTM D3330 standard on a Computerized Servo System Peel Strength Tester (Dongguan Kejian Instrument Co., Ltd., China) at a peeling speed of 300 mm/min. The peel adhesion was defined as the average value of five tests.

Small-Angle X-Ray Scattering Experiment. Copolymer films with 50 μm thickness were used in the SAXS experiment. The X-ray diffraction data were recorded at beamline BL16B1 of the Shanghai Synchrotron Radiation Facility (SSRF) at a wavelength of 1.2398 Å. Beamline BL16B1 is based on a bending magnet and a Si (111) double-crystal monochromator was employed to monochromatize the beam. The spot size was 0.39 × 0.48 mm^2 and a Pilatus 200 K-A detector was used for data collection. A silver(I) behenate standard sample was determined for the d-spacing calibration. The one-dimensional (1D) circular integrations of two-dimensional (2D) SAXS patterns were performed using the Igor Pro 6.37 (with Nika 2D SAS macros) software package.

Rheology Characterization (Creep, Temperature Swipe, Frequency Scan). The viscoelastic behavior of the H-copolymers was evaluated using a TA Instruments DHR-2 rheometer equipped with an 8 mm diameter parallel round plate and an ∼1000 μm gap for all rheological experiments.

The creep recovery experiments were performed by applying a 20 kPa shear force on the samples for 10 min at 25 °C and then removing the shear force immediately to record the following 10 min recovery of the sample. The rheology properties at different temperatures were characterized by performing temperature ramps from −50 to 120 °C with a heating rate of 3 °C/min and 0.2% shear force at a frequency of 1 Hz. Frequency scans were obtained by subjecting the samples to oscillatory shear rates (500−0.05 rad/s) in the linear viscoelastic regime (1.0% strain) over the temperature range of −20 to +80 °C in 10 °C increments. The master curves at a reference temperature of 30 °C were generated using time−temperature superposition (TTS) via the commercially available software package TRIOS (TA Instruments) by using the Williams−Landel−Ferry (WLF) equation.

Gel Fraction Test. The gel fraction, which represents the degree of cross-linking of the copolymer, was measured by putting the cross-linked copolymer in toluene for 12 h twice, and the insoluble gel was then filtered and dried at 80 °C in a vacuum. The gel fraction was the mass ratio of copolymers before and after dissolution in toluene.

■ ASSOCIATED CONTENT

Supporting Information

The Supporting Information is available free of charge at https://pubs.acs.org/doi/10.1021/acsomega.3c07566.

Detailed synthesis and ^{1}H NMR; ^{13}C NMR data of H-monomers (Figures S1−S14); the DSC curves of H-homopolymers (Figure S15); TGA data of H-copolymers were recorded in (Figure S16); ^{1}H NMR spectra of H-copolymers were shown in (Figures S17−S19); plot of K_a (H-monomers) and T_g (homopolymers) (Figure S20 and Table S1); the raw theology master curve data of un-cross-linked H-copolymers (Figure S21); the master curves of un-cross-linked pEHA and $pAA_{10}EHA_{90}$ (Figure S22) (PDF)

■ AUTHOR INFORMATION

Corresponding Author

Jianhui Xia − *South China Advanced Institute for Soft Matter Science and Technology, School of Emergent Soft Matter, Guangdong Provincial Key Laboratory of Functional and Intelligent Hybrid Materials and Devices, South China University of Technology, Guangzhou 510640, China;* orcid.org/0000-0002-8857-3879; Email: xiajh@scut.edu.cn

Author

Weizhong Xiang − *South China Advanced Institute for Soft Matter Science and Technology, School of Emergent Soft Matter, Guangdong Provincial Key Laboratory of Functional and Intelligent Hybrid Materials and Devices, South China*

https://doi.org/10.1021/acsomega.3c07566
ACS Omega 2024, 9, 13644−13654

University of Technology, Guangzhou 510640, China; orcid.org/0009-0007-5988-3775

Complete contact information is available at: https://pubs.acs.org/10.1021/acsomega.3c07566

Notes

The authors declare no competing financial interest.

■ ACKNOWLEDGMENTS

This research is supported by the Guangdong Provincial Key Laboratory of Functional and Intelligent Hybrid Materials and Devices (No. 2019B121203003), Major Program of National Natural Science Foundation of China (No. 51890871), and The Recruitment Program of Guangdong (No. 2016ZT06C322). The author thanks Dr. Leo for useful discussions and contribution on the SAXS experiments.

■ REFERENCES

(1) Wu, D.; Shi, J.; Chen, J.; Liao, D. In *P-10.3: Structural Optimization Method of Foldable AMOLED Panel Based on Mechanical Theory*, SID Symposium Digest of Technical Papers; Wiley Online Library, 2021; pp 574−577.

(2) Cheng, A.; Chen, Y.; Jin, J.; Su, T. In *74-3: Study on Mechanical Behavior and Effect of Adhesive Layers in Foldable AMOLED Display by Finite Element Analysis*, SID Symposium Digest of Technical Papers; Wiley Online Library, 2019; pp 1060−1063.

(3) Fang, Y.; Xia, J. Highly Stretchable, Soft, and Clear Viscoelastic Film with Good Recoverability for Flexible Display. *ACS Appl. Mater. Interfaces* **2022**, *14* (33), 38398−38408.

(4) Han, S. H.; Shin, J. H.; Choi, S. S. Analytical investigation of multi-layered rollable displays considering nonlinear elastic adhesive interfaces. *Sci. Rep.* **2023**, *13* (1), No. 5697.

(5) Droesbeke, M. A.; Aksakal, R.; Simula, A.; Asua, J. M.; Du Prez, F. E. Biobased acrylic pressure-sensitive adhesives. *Prog. Polym. Sci.* **2021**, *117*, No. 101396, DOI: 10.1016/j.progpolymsci.2021.101396.

(6) Callies, X.; Herscher, O.; Fonteneau, C.; Robert, A.; Pensec, S.; Bouteiller, L.; Ducouret, G.; Creton, C. Combined Effect of Chain Extension and Supramolecular Interactions on Rheological and Adhesive Properties of Acrylic Pressure-Sensitive Adhesives. *ACS Appl. Mater. Interfaces* **2016**, *8* (48), 33307−33315.

(7) Kuo, C. F. J.; Chen, J. B.; Chang, S. H. Low corrosion optically clear adhesives for conducting glass: I. Effects of N, N-diethylacrylamide and acrylic acid mixtures on optically clear adhesives. *J. Appl. Polym. Sci.* **2018**, *135* (21), No. 46277.

(8) Lee, J. H.; Park, J.; Myung, M. H.; Baek, M.-J.; Kim, H.-S.; Lee, D. W. Stretchable and recoverable acrylate-based pressure sensitive adhesives with high adhesion performance, optical clarity, and metal corrosion resistance. *Chem. Eng. J.* **2021**, *406*, No. 126800.

(9) Xie, Z.; Hu, B.-L.; Li, R.-W.; Zhang, Q. Hydrogen Bonding in Self-Healing Elastomers. *ACS Omega* **2021**, *6* (14), 9319−9333.

(10) Chen, J.; Liu, J.; Thundat, T.; Zeng, H. Polypyrrole-doped conductive supramolecular elastomer with stretchability, rapid self-healing, and adhesive property for flexible electronic sensors. *ACS Appl. Mater. Interfaces* **2019**, *11* (20), 18720−18729.

(11) Zhang, C.; Yang, Z.; Duong, N. T.; Li, X.; Nishiyama, Y.; Wu, Q.; Zhang, R.; Sun, P. Using Dynamic Bonds to Enhance the Mechanical Performance: From Microscopic Molecular Interactions to Macroscopic Properties. *Macromolecules* **2019**, *52* (13), 5014−5025.

(12) Das, S.; Samitsu, S.; Nakamura, Y.; Yamauchi, Y.; Payra, D.; Kato, K.; Naito, M. Thermo-resettable cross-linked polymers for reusable/removable adhesives. *Polym. Chem.* **2018**, *9* (47), 5559−5565.

(13) Mozhdehi, D.; Neal, J. A.; Grindy, S. C.; Cordeau, Y.; Ayala, S.; Holten-Andersen, N.; Guan, Z. Tuning Dynamic Mechanical Response in Metallopolymer Networks through Simultaneous Control of Structural and Temporal Properties of the Networks. *Macromolecules* **2016**, *49*, 6310−6321.

(14) Zhang, Z.; Ghezawi, N.; Li, B.; Ge, S.; Zhao, S.; Saito, T.; Hun, D.; Cao, P. F. Autonomous Self-Healing Elastomers with Unprecedented Adhesion Force. *Adv. Funct. Mater.* **2021**, *31* (4), No. 2006298.

(15) Xu, S.; Zhao, B.; Raza, M.; Li, L.; Wang, H.; Zheng, S. Shape Memory and Self-Healing Nanocomposites with POSS−POSS Interactions and Quadruple Hydrogen Bonds. *ACS Appl. Polym. Mater.* **2020**, *2* (8), 3327−3338.

(16) Shen, J.; Chen, T.; Huang, Y.; Jin, Q.; Ji, J. New Morphogenetic Strategy Inspired by the Viscoelasticity of Polymers. *ACS Appl. Mater. Interfaces* **2020**, *12* (32), 36620−36627, DOI: 10.1021/acsami.0c08995.

(17) Heinzmann, C.; Salz, U.; Moszner, N.; Fiore, G. L.; Weder, C. Supramolecular cross-links in poly (alkyl methacrylate) copolymers and their impact on the mechanical and reversible adhesive properties. *ACS Appl. Mater. Interfaces* **2015**, *7* (24), 13395−13404.

(18) Heinzmann, C.; Lamparth, I.; Rist, K.; Moszner, N.; Fiore, G. L.; Weder, C. Supramolecular Polymer Networks Made by Solvent-Free Copolymerization of a Liquid 2-Ureido-4 [1 H]-pyrimidinone Methacrylamide. *Macromolecules* **2015**, *48* (22), 8128−8136.

(19) Balkenende, D. W. R.; Winkler, S. M.; Li, Y.; Messersmith, P. B. Supramolecular Cross-Links in Mussel-Inspired Tissue Adhesives. *ACS Macro Lett.* **2020**, *9* (10), 1439−1445.

(20) Sijbesma, R. P.; Beijer, F. H.; Brunsveld, L.; Folmer, B. J.; Hirschberg, J. K.; Lange, R. F.; Lowe, J. K.; Meijer, E. Reversible polymers formed from self-complementary monomers using quadruple hydrogen bonding. *Science* **1997**, *278* (5343), 1601−1604.

(21) de Greef, T. F. A.; Nieuwenhuizen, M. M.; Sijbesma, R. P.; Meijer, E. Competitive intramolecular hydrogen bonding in oligo (ethylene oxide) substituted quadruple hydrogen bonded systems. *J. Org. Chem.* **2010**, *75* (3), 598−610.

(22) Moon, H.; Jeong, K.; Kwak, M. J.; Choi, S. Q.; Im, S. G. Solvent-free deposition of ultrathin copolymer films with tunable viscoelasticity for application to pressure-sensitive adhesives. *ACS Appl. Mater. Interfaces* **2018**, *10* (38), 32668−32677.

(23) Sadeghzade, S.; Cao, J.; Zhang, D.; Dong, P.; Hu, J.; Es'haghioskui, A.; Yuan, H. Soft acrylate monomer-based optically clear adhesive for foldable electronics: Mechanical characterization and fractography analysis under large strain. *Eur. Polym. J.* **2023**, *197*, No. 112337.

(24) Lin, S.-T.; Liu, C.-Y.; Lu, Y.-Y.; Su, W.-C. Acrylamide or (Meth)acrylamide-Containing High Tg Additive for Pressure Sensitive Adhesives. WO Patent WO074,562A1, 2022.

(25) Ballard, N. Supramolecularly Reinforced Films from Polyurethane−Urea Dispersions Containing the Tris-Urea Motif. *ACS Appl. Polym. Mater.* **2020**, *2* (9), 4045−4053.

(26) Zhou, Y. N.; Li, J.; Wu, Y.; Luo, Z. H. Role of External Field in Polymerization: Mechanism and Kinetics. *Chem. Rev.* **2020**, *120* (5), 2950−3048.

(27) Ni, Y.; Becquart, F.; Chen, J.; Taha, M. Polyurea−Urethane Supramolecular Thermo-Reversible Networks. *Macromolecules* **2013**, *46* (3), 1066−1074.

(28) Xu, J.; Chen, W.; Wang, C.; Zheng, M.; Ding, C.; Jiang, W.; Tan, L.; Fu, J. Extremely stretchable, self-healable elastomers with tunable mechanical properties: Synthesis and applications. *Chem. Mater.* **2018**, *30* (17), 6026−6039.

(29) Kim, S. M.; Jeon, H.; Shin, S. H.; Park, S. A.; Jegal, J.; Hwang, S. Y.; Oh, D. X.; Park, J. Superior toughness and fast self-healing at room temperature engineered by transparent elastomers. *Adv. Mater.* **2018**, *30* (1), No. 1705145.

(30) Jansen, J. F. G. A.; Dias, A. A.; Dorschu, M.; Coussens, B. Fast Monomers: Factors Affecting the Inherent Reactivity of Acrylate Monomers in Photoinitiated Acrylate Polymerization. *Macromolecules* **2003**, *36* (11), 3861−3873.

(31) Berchtold, K. A.; Nie, J.; Stansbury, J. W.; Bowman, C. N. Reactivity of monovinyl (meth) acrylates containing cyclic carbonates. *Macromolecules* **2008**, *41* (23), 9035−9043.

(32) Wang, Y.-J.; He, Y.; Zheng, S. Y.; Xu, Z.; Li, J.; Zhao, Y.; Chen, L.; Liu, W. Polymer Pressure-Sensitive Adhesive with A Temperature-Insensitive Loss Factor Operating Under Water and Oil. *Adv. Funct. Mater.* **2021**, *31* (48), No. 2104296.
(33) Amemori, S.; Kokado, K.; Sada, K. Fundamental Molecular Design for Precise Control of Thermoresponsiveness of Organic Polymers by Using Ternary Systems. *J. Am. Chem. Soc.* **2012**, *134* (20), 8344−8347.
(34) Cheng, S.; Zhang, M.; Dixit, N.; Moore, R. B.; Long, T. E. Nucleobase Self-Assembly in Supramolecular Adhesives. *Macromolecules* **2012**, *45* (2), 805−812.
(35) Chen, M.; Inglefield, D. L.; Zhang, K.; Hudson, A. G.; Talley, S. J.; Moore, R. B.; Long, T. E. Synthesis of urea-containing ABA triblock copolymers: Influence of pendant hydrogen bonding on morphology and thermomechanical properties. *J. Polym. Sci., Part A: Polym. Chem.* **2018**, *56* (16), 1844−1852.
(36) Woodward, P. J.; Merino, D. H.; Greenland, B. W.; Hamley, I. W.; Light, Z.; Slark, A. T.; Hayes, W. Hydrogen Bonded Supramolecular Elastomers: Correlating Hydrogen Bonding Strength with Morphology and Rheology. *Macromolecules* **2010**, *43* (5), 2512−2517.
(37) Zhang, K.; Aiba, M.; Fahs, G. B.; Hudson, A. G.; Long, T. E.; et al. Nucleobase-Functionalized Acrylic ABA Triblock Copolymers and Supramolecular Blends. *Polym. Chem.* **2015**, *6* (13), 2434−2444.
(38) Yamauchi, K.; Lizotte, J. R.; Long, T. E. Thermoreversible Poly(alkyl acrylates) Consisting of Self-Complementary Multiple Hydrogen Bonding. *Macromolecules* **2003**, *36* (4), 1083−1088.
(39) Zhang, K.; Fahs, G. B.; Aiba, M.; Moore, R. B.; Long, T. E. Nucleobase-functionalized ABC triblock copolymers: self-assembly of supramolecular architectures. *Chem. Commun.* **2014**, *50* (65), 9145−9148.
(40) de Greef, T. F. A.; Nieuwenhuizen, M. M. L.; Stals, P. J. M.; Fitié, C. F. C.; Palmans, A. R. A.; Sijbesma, R. P.; Meijer, E. W. The influence of ethylene glycol chains on the thermodynamics of hydrogen-bonded supramolecular assemblies in apolar solvents. *Chem. Commun.* **2008**, No. 36, 4306−4308.
(41) Yuan, Y.; Li, C.; Zhang, R.; Liu, R.; Liu, J. Low volume shrinkage photopolymerization system using hydrogen-bond-based monomers. *Prog. Org. Coat.* **2019**, *137*, No. 105308.
(42) Chen, T. T. D.; Carrodeguas, L. P.; Sulley, G. S.; Gregory, G. L.; Williams, C. K. Bio-based and Degradable Block Polyester Pressure-Sensitive Adhesives. *Angew. Chem., Int. Ed.* **2020**, *59* (52), 23450−23455.
(43) Shabbir, A.; Javakhishvili, I.; Cerveny, S.; Hvilsted, S.; Skov, A. L.; Hassager, O.; Alvarez, N. J. Linear viscoelastic and dielectric relaxation response of unentangled UPy-based supramolecular networks. *Macromolecules* **2016**, *49* (10), 3899−3910.
(44) Lewis, C. L.; Stewart, K.; Anthamatten, M. The influence of hydrogen bonding side-groups on viscoelastic behavior of linear and network polymers. *Macromolecules* **2014**, *47* (2), 729−740.
(45) Shabbir, A.; Goldansaz, H.; Hassager, O.; Ruymbeke, E. V.; Alvarez, N. J. Effect of Hydrogen Bonding on Linear and Nonlinear Rheology of Entangled Polymer Melts. *Macromolecules* **2015**, *48* (16), 5988−5996.
(46) Golkaram, M.; Csaba, F.; Evelyne, V. R.; Katja, L. Linear Viscoelasticity of Weakly Hydrogen-Bonded Polymers near and below the Sol−Gel Transition. *Macromolecules* **2018**, *51*, 4910−4916.
(47) Giubertoni, G.; Burla, F.; Bakker, H. J.; et al. Connecting the Stimuli-Responsive Rheology of Biopolymer Hydrogels to Underlying Hydrogen-Bonding Interactions. *Macromolecules* **2020**, *53*, 10503−10513.
(48) Lei, L.; Xia, Z.; Ou, C.; Zhang, L.; Zhong, L. Effects of crosslinking on adhesion behavior of waterborne polyurethane ink binder. *Prog. Org. Coat.* **2015**, *88*, 155−163.
(49) Czech, Z.; Milker, R. Solvent-free radiation-curable polyacrylate pressure-sensitive adhesive systems. *J. Appl. Polym. Sci.* **2003**, *87*, 182−191.

https://doi.org/10.1021/acsomega.3c07566
ACS Omega 2024, 9, 13644−13654